0026-895X/04/6603-420–429$20.00
MOLECULAR PHARMACOLOGY
Copyright © 2004 The American Society for Pharmacology and Experimental Therapeutics
Mol Pharmacol 66:420–429, 2004

Vol. 66, No. 3
59/1172369
Printed in U.S.A.

The α7 Nicotinic Acetylcholine Receptor Subunit Exists in Two Isoforms that Contribute to Functional Ligand-Gated Ion Channels

Emily G. Severance, Hongling Zhang, Yolmari Cruz, Sergei Pakhlevaniants, Stephen H. Hadley, Jahanshah Amin, Lynn Wecker, Crystal Reed, and Javier Cuevas

Department of Pharmacology and Therapeutics, University of South Florida College of Medicine, Tampa, Florida

Received March 4, 2004; accepted June 17, 2004

ABSTRACT

Fast synaptic transmission in mammalian autonomic ganglia is mediated primarily by nicotinic receptors, and one of the most abundant nicotinic acetylcholine receptor subtypes in these neurons contains the α7 subunit (α7-nAChRs). Unlike α7-nAChRs expressed in other cells, the predominant α7-nAChR subtype found in rat intracardiac and superior cervical ganglion neurons exhibits a slow rate of desensitization and is reversibly blocked by α-bungarotoxin (αBgt). We report here the identification of an α7 subunit sequence variant in rat autonomic neurons that incorporates a novel 87-base pair cassette exon in the N terminus of the receptor and preserves the reading frame of the transcript. This α7 isoform was detected using reverse transcriptase-polymerase chain reaction techniques in neonatal rat brain and intracardiac and superior cervical ganglion neurons. Immunoblot experiments using a polyclonal antibody directed against the deduced amino acid sequence of the α7-2 insert showed a pattern of expression consistent with α7-2 subunit mRNA distribution. Moreover, the α7-2 subunit could be immunodepleted from protein extracts by solid-phase immunoprecipitation techniques using the anti-α7 monoclonal antibody 319. The α7-2 subunit was shown to form functional homomeric ion channels that were activated by acetylcholine and blocked by α-bungarotoxin when expressed in *Xenopus laevis* oocytes. This α7 isoform exhibited a slow rate of desensitization, and inhibition of these channels by αBgt reversed rapidly after washout. Taken together, these data indicate that the α7-2 subunit is capable of forming functional αBgt-sensitive acetylcholine receptors that resemble the α7-nAChRs previously identified in rat autonomic neurons. Furthermore, the distribution of the α7-2 isoform is not limited to peripheral neurons.

Nicotinic acetylcholine receptor channels (nAChRs) that contain the α7 gene product (α7-nAChRs) are one of the most abundant types of nicotinic receptors in the vertebrate nervous system. The α7-nAChRs differ from most neuronal nicotinic receptors in that they bind α-bungarotoxin (αBgt) with high affinity and have calcium permeability comparable with glutamatergic *N*-methyl-D-aspartate receptors (Seguela et al., 1993). The α7-nAChRs modulate various cell processes ranging from synaptic transmission (Zhang et al., 1996) to apoptosis (Berger et al., 1998). In the central nervous system, these receptors seem to be involved in learning and memory (Radcliffe and Dani, 1998) and have been linked to pathophysiological conditions such as schizophrenia (Freedman et al., 1997). Experiments have also shown that the β-amyloid peptide is a ligand for α7-nAChRs (Liu et al., 2001; Dineley et al., 2002), suggesting that α7-nAChR function may be altered during Alzheimer's disease. Furthermore, the α7-nAChRs participate in important physiological processes in the viscera, such as the regulation of inflammation (Wang et al., 2003) and nicotine-induced nitrergic neurogenic vasodilation (Si and Lee, 2002).

The α7 nicotinic acetylcholine receptor subunit was first cloned from chick brain (Schoepfer et al., 1990). This subunit was later found to form functional homomeric AChRs when expressed in *Xenopus laevis* oocytes (Seguela et al., 1993) and to contribute to functional nAChRs in native cells (Alkondon and Albuquerque, 1993; Zhang et al., 1994). Although there is strong evidence that native α7-nAChRs are homopentamers (Chen and Patrick, 1997; Drisdel and Green, 2000), the composition and stoichiometry of native α7-nAChRs remains

This work was supported by National Institutes of Health grant HL63247 (to J.C.).
Article, publication date, and citation information can be found at http://molpharm.aspetjournals.org.
doi:10.1124/mol.104.000059.

ABBREVIATIONS: nAChR, nicotinic acetylcholine receptor; α7-nAChR, nicotinic acetylcholine receptor containing the α7 gene product; αBgt, α-bungarotoxin; bp, base pair; RT-PCR, reverse transcriptase-polymerase chain reaction; ACh, acetylcholine; SCG, superior cervical ganglia; PCR, polymerase chain reaction; ICG, intracardiac ganglia; Ab, antibody; mAb, monoclonal antibody.

to be confirmed. For example, the α7 subunit can combine with the β2 subunit to form functional heteropentamers in *X. laevis* oocytes (Khiroug et al., 2002), and the widespread coexpression of these two subunits in the central nervous system has led investigators to suggest that they may form such heteropentamers in vivo (Azam et al., 2003). In addition, differences exist in the pharmacological and biophysical properties of α7-nAChRs from a variety of cell types, an indication of variability in the structure or subunit composition of α7-nAChRs. For example, whereas α7-nAChRs in rat hippocampal neurons desensitize rapidly and bind αBgt in an irreversible manner (Alkondon and Albuquerque, 1993), α7-nAChRs in mammalian autonomic neurons desensitize slowly and recover rapidly from αBgt blockade (Cuevas and Berg, 1998; Cuevas et al., 2000). More recently, denervated mouse muscle was shown to express a subtype of α7-AChRs that desensitizes slowly and is not blocked by the classic α7-AChR–selective antagonist methyllycaconitine (Tsuneki et al., 2003).

Cuevas and Berg (1998) proposed that the heterogeneity in α7-nAChRs might be caused by cell-dependent expression of α7 subunit isoforms. This theory was supported by the observation that splice variations of the α7 subunit are detected in human brain and leukocytes (Gault et al., 1998; Villiger et al., 2002). However, most of these α7 isoforms contain a premature stop codon (Gault et al., 1998) or form a truncated subunit that is not activated by acetylcholine (Villiger et al., 2002). Although various other ligand-gated ion channels such as 5-hydroxytryptamine-3 and GABA receptors express functional splice variants with distinct properties (Bruss et al., 2000), this type of diversity has been less forthcoming in nicotinic acetylcholine receptors.

In the current study, we present the first evidence for a functional splice variant of a nicotinic receptor subunit that contributes to a distinctive channel. The α7-2 isoform of the α7 nicotinic receptor subunit contains an 87-base pair insert that represents the incorporation of a novel exon (exon 4a) between exons 4 and 5 of the conventional α7 gene product (α7-1). The α7-2 splice variant is expressed in both peripheral and central neurons, and when expressed in *X. laevis* oocytes, it produces functional ACh-gated ion channels. The biophysical and pharmacological properties of the homomeric channel formed by α7-2 differ from those of homomeric α7-1–nAChRs and resemble those of the slowly desensitizing α7-nAChRs of rat autonomic neurons.

Materials and Methods

RT-PCR. The expression of α7 nicotinic receptor subunit splice variants in central and peripheral neurons was examined using RT-PCR techniques similar to those reported previously (Zhang and Cuevas, 2002). Total RNA was isolated from rat intracardiac ganglia and associated tissue, superior cervical ganglia (SCG), nodosal ganglia and brain (RNeasy; QIAGEN GmbH, Hilden, Germany). Primers specific for the α7 gene product (α7-P1) were designed to span an intron to discriminate between genomic DNA and cDNA. Table 1 lists the sequences of the primers used in this study and the predicted size for the products. For single-cell RT-PCR experiments, intracardiac neurons were dissociated from 4- to 7-day-old neonatal rats, and cytoplasm was extracted from isolated neurons as described previously (Zhang and Cuevas, 2002). All procedures were done in accordance with the regulations of the University of South Florida Institutional Animal Care and Use Committee. Negative controls for these experiments included the use of water as template for the RT-PCR and the suctioning of extracellular solution to control for cytoplasmic contamination in the single-cell RT-PCR reactions. PCR products were gel-purified using a QIAEX II Gel Purification kit (QIAGEN) and sequenced by the Molecular Biology Core Facility at the H. Lee Moffitt Cancer Center and Research Institute (University of South Florida, Tampa, FL).

The relative abundance of α7-1 and α7-2 isoforms in central and peripheral tissues was determined using the α7-P5 primer combination (Table 1) containing two forward primers, one selective for both isoforms and a second that specifically amplifies α7-2 transcripts, and a reverse primer that recognizes both α7 splice variants. This primer combination was used to overcome preferential amplification of the smaller α7-1 transcripts, which would occur if only a single primer pair, such as α7-P1 was used. The ability of this primer pair to properly detect the relative abundance of α7-1 and α7-2 transcripts was assessed by using various ratios of α7-1- and α7-2-pCIneo plasmids (1:10 to 10:1) and was linear over the range tested.

Genomic DNA Extraction and PCR Amplification. Genomic DNA was isolated from the livers of 7-day-old neonatal rats using the Wizard Genomic DNA Purification Kit (Promega, Madison, WI). Rats were killed by decapitation for these experiments. Primer pairs

TABLE 1

Sequence of oligonucleotide primers used in this study, and the predicted size for the individual products

Primers specific for the splice insert are shown in bold italics. Nucleotide numbers correspond to the sequence of the RATNARAD (accession number L31619) in Fig. 2, except for those that are specific for the α7-2 (bold italics), which correspond to the nucleotide numbers used for the splice variant in Fig. 2. Product sizes shown in bold italics represent the diagnostic bands used to determine relative abundance of the α7-1 and α7-2 isoforms.

Name	Sequence	Nucleotide Numbers	Product Size
			bp
α7-P1			
Forward	GTACAAGGAGCTGGTCAAGAACTACAACC	109–137	740(α7-2)
Reverse	GGGCTGAAATGAGTACACAAGG	740–761	653(α7-1)
α7-P2			
Forward	GGAGTGAAGAATGTTCGTTTTCCAG	308–332	91(α7-2)
Reverse	***CTTGGTCAAAATGCAACTGACACC***	***375–398***	
α7-P3			
Forward	***AGTTGCATTTTGACCAAGATCTGC***	***381–404***	122(α7-2)
Reverse	CAAAACATTGGTGTGGAACGTG	394–415	
α7-P4			
Forward	***GGTGTCAGTTGCATTTTGACCAAG***	***375–398***	474(α7-2)
Reverse	GGGCTGAAATGAGTACACAAGG	740–761	
α7-P5			
Forward	GTACAAGGAGCTGGTCAAGAACTACAACC	109–137	740(α7-1)
Forward	***AGTTGCATTTTGACCAAGATCTGC***	***381–404***	***653(α7-1)***
Reverse	GGGCTGAAATGAGTACACAAGG	740–761	***468(α7-2)***

were designed to detect the presence of introns flanking the putative exon 4a of the rat α7 gene. One primer pair, α7-P2, consisted of a sense primer located in exon 4 and an antisense primer that was specific to the insert of the α7-2 variant. A second primer pair, α7-P3, consisted of a sense primer specific for the α7-2 insert and an antisense primer specific for exon 5. Genomic DNA was amplified by PCR in 50-μl reactions containing 1× PCR buffer, 2.0 mM $MgCl_2$, 0.2 mM each dNTP, 0.2 μM each primer, and 1.25 units of HotStarTaq polymerase (QIAGEN). A negative control that lacked template DNA was also included. PCR products were electrophoresed through a 1% Tris/borate/EDTA agarose gel, stained with ethidium bromide, and visualized through UV illumination.

Immunoblot Analysis. Whole brains and SCG were dissected from 10- to 14-day-old neonatal rats, and intracardiac ganglia (ICG) were dissected from postnatal day 1 to 5 rats. For brain and intracardiac ganglia dissections, animals were killed by decapitation, and they were killed by CO_2 asphyxiation for SCG dissections. Tissues were homogenized in a 2% Triton X-100 extraction buffer containing 50 mM sodium phosphate, pH 7.4, and the following protease inhibitors: 0.4 mM iodoacetamide, 5 mM benzamidine, 5 μg/ml phosphoramidon, 10 μg/ml soybean trypsin inhibitor, 10 μg /ml leupeptin, 20 μg /ml pepstatin A, 5 mM EDTA, 5 mM EGTA, 2 μg/ml aprotinin, and 1 mM phenylmethylsulfonyl fluoride; they were then incubated for 1 h at 4°C before centrifuging. Homogenates were sedimented at 15,000 rpm for 15 min at 4°C, and the supernatant were centrifuged at 33,000 rpm for 1 h at 4°C. The supernatant containing the detergent extracts was collected and stored at −20°C before experiments.

Protein concentrations of the detergent extracts were determined using the Bio-Rad Protein Assay I (Bio-Rad, Hercules, CA). For immunodepletion, AChRs were immunotethered to microtiter wells in a manner described previously for solid-phase immunoprecipitations (Conroy and Berg, 1995; Cuevas et al., 2000). Equal amounts of extract were incubated overnight with constant agitation at 4°C in wells containing a 1:1000 dilution of the α7 subunit-specific mAb 319 (Sigma/RBI, Natick, MA) anchored with rabbit–anti-rat IgG (depleted) or in wells containing only rabbit–anti-rat IgG (mock-depleted control). In some experiments donkey–anti-rabbit was used as the anchoring antibody. As a negative control, solubilization buffer (with no protein) was incubated in the antibody-coated microtiter wells and tested for immunoreactivity. Proteins were resolved on a 10% SDS-polyacrylamide gel electrophoresis and electroblotted to polyvinylidene difluoride (Immobilon P; Millipore Corporation, Billerica, MA). Membranes were blocked with 5% nonfat dried milk and then probed with a rabbit anti-α7-2 polyclonal antibody, Ab 87 (diluted 1:50), generated against a fusion peptide with sequence identical to the deduced amino acid sequence of exon 4a (FabGennix, Inc., Shreveport, LA). After secondary antibody incubation, signals were detected with chemiluminescent visualization (ECL; Santa Cruz Biotechnology, Inc., Santa Cruz, CA). The specificity of the Ab 87 polyclonal antibody for α7-2 relative to α7-1 was assessed using protein extracts from SH-EP1 cells stably transfected with the α7-1 subunit. Whereas a ~55-kilobase product was readily detected in the extracts using the anti-α7-1 mAb 319, no such product was observed when blots were probed with Ab 87 (data not shown). No bands were detected in immunoblots of blank experiments.

Oocyte Recordings. Intrinsic cardiac neuron RNA extracts were amplified by RT-PCR using the primers α7-P1, and the resulting α7-2 cDNA was gel-purified (Gel Extraction Kit; QIAGEN). The full-length α7-2 subunit was then generated by splicing the α7-2 cDNA into a rat α7-1 clone using the restriction enzymes Cfr101 and Eco47III (Roche Diagnostics, Indianapolis, IN). Both α7-1 and α7-2 subunit cDNAs (in pCI-neo) were linearized with the restriction enzyme NotI, transcribed and $m^7G(5')ppp(5')$G-capped using a Megascript Kit (Ambion, Austin, TX). Integrity and yield of the cRNA was verified on a 1% formaldehyde agarose gel.

X. laevis (Xenopus I, Ann Arbor, MI) were anesthetized using tricaine methane sulfonate, and oocytes were surgically removed from the frog and placed in a solution that consisted of 82.5 mM NaCl, 2.5 mM KCl, 10 mM HEPES, 2 mM $CaCl_2$, 1 mM $MgCl_2$, 10 mM Na_2HPO_4, 50 U/ml penicillin, and 50 μg/ml streptomycin, pH 7.5. Oocytes were dispersed in this same solution minus Ca^{2+} and plus 0.3% collagenase A (Roche Diagnostics) and rinsed, and stage VI oocytes were separated and maintained overnight at 18°C. Micropipettes for injection of cRNA were pulled on a Sutter P87 horizontal puller (Sutter Instrument Company, Novato, CA). Approximately 10 to 50 ng of α7-2 cRNA was injected into the oocytes by applying positive pressure using a Picospritzer II (General Valve, Fairfield, NJ).

Recordings were conducted 3 to 7 days after injection. Oocytes were placed in a small volume chamber (<100 μl) and continuously perfused via a 1.5-mm glass pipette positioned ~1 mm from the oocyte. The glass pipette was connected to a low-volume MP-8 perfusion manifold (Warner Instrument, Hamden, CT), permitting rapid solution change (<1 s). Solutions were applied via gravity feed regulated by solenoid valves (Parker-Hannifin, Cleveland, OH) controlled by a valve driver (Parker-Hannifin) and a Master 8 TTL pulse generator (AMPI, Jerusalem, Israel). Recording microelectrodes with a final resistance of 1 to 3 μΩ were fabricated with Narishige PP-83 puller (Narishige, East Meadow, NY) and filled with 3 M KCl. Standard two-electrode voltage-clamp techniques were used to record currents in response to agonist application. Data were amplified using a Geneclamp 500B amplifier, digitized at 5 kHz with a Digidata 1322A digitizer, and recorded and analyzed on a computer using the pClamp 9 programs (all from Axon Instruments, Union City, CA).

The control external solution for voltage-clamp recordings consisted of 115 mM NaCl, 2.5 mM KCl, 1.8 mM $BaCl_2$, and 10 mM HEPES, pH 7.2. This solution limited the activation and thus the contamination of our recordings by calcium-activated chloride currents expressed in *X. laevis* oocytes (Seguela et al., 1993; Peng et al., 1994). Ca^{2+} was isosmotically substituted for Ba^{2+} in the indicated experiments (calcium-physiological salt solution). The recording chamber was continuously perfused (10 ml/min), and drugs were applied using the application system described above.

Results

To test the hypothesis that rat intracardiac neurons express splice variants of the α7 gene product, intrinsic cardiac neurons were studied using RT-PCR techniques. Oligonucleotide primers (α7-P1) (Table 1) were designed to amplify a 653-bp region corresponding to nucleotide positions 109 to 761 of the *Rattus norvegicus* nicotinic acetylcholine receptor α7 subunit mRNA (accession number L31619). This region is known to encode the extracellular domain containing both the αBgt and competitive agonist binding sites (Brejc et al., 2001). Several products with sizes ranging from 400 to 750 bp were detectable over the course of these experiments (Fig. 1A) ($n > 10$). Cloning and sequencing of the products indicated that several of these products represented splice variants of the α7 gene.

The conventional α7 gene product (α7-1) (Fig. 1A) is composed of 10 exons, with the first transmembrane domain encoded in exon 7 (Fig. 1B). Three of the α7 splice variants detected in intrinsic cardiac neurons were the result of deletions of all or parts of exons 3 to 6 (Fig. 1C). All of these splice variants resulted in a frame shift and contained a premature stop codon before the region encoding the competitive agonist-binding site. The fourth splice variant (α7-2) (Fig. 1A) contains an 87-bp insert between the regions encoded by exons 4 and 5 (Fig. 1C). Figure 2 shows the sequence of the insert contributing to α7-2 and flanking regions aligned to the conventional α7 gene product (accession number

L31619). The insert preserves the reading frame of the transcripts, and the deduced amino acid sequence is provided in Fig. 2. The predicted protein sequence for the insert was analyzed using multiple algorithms on the Network Protein Sequence @nalysis Server (Lyon, France). Results suggest that the secondary structure of the domain encoded by the α7-2 insert is an α helix flanked by random coils (data not shown).

To determine whether the 87-bp insert represents a shift in the donor or acceptor sites of exon 4 and/or exon 5, respectively, rat genomic DNA was probed using primers specific for the insert and flanking sequences (α7-P2 and α7-P3) (Table 1). Primer pair α7-P2 has a forward primer specific for exon 4 and a reverse primer specific for the α7-2 insert, whereas primer pair α7-P3 has a forward primer specific for the insert and a reverse primer specific for exon 5. With primer set, α7-P2, a 505-bp product, was detected that when sequenced included sequentially 5′ to 3′, exon 4, a putative 413-bp intron, and the α7-2 insert (Fig. 3). This genomic sequence aligned to the α7-2 splice variant cDNA sequence is shown in Fig. 4. Consistent with an intron, the 413-bp section contains consensus donor and acceptor sequences at the 5′ and 3′ ends, respectively (Fig. 4). Amplification of genomic DNA using primers α7-P3, specific for the α7-2 insert and the 3′ flanking exon 5, failed to yield any product even though these primers could readily amplify cDNA encoding the α7-2 splice variant (Fig. 4) (cDNA, α7-P3). Intron 4 in the rat α7 gene is known to be >25,000 bp (National Center for Biotechnology Information, Entrez Rat Genome, National Library of Medicine, Bethesda, MD), and such a large product would not have been detected by our methods, thus explaining the lack of product in our genomic DNA PCR reaction. Taken together, these data suggest that the α7-2 splice variant is produced via the incorporation of a novel exon, exon 4a, and the α7 gene. Experiments were also conducted to determine whether any other sequence variations in the α7 gene product are linked with the exon 4a cassette insert. RT-PCR analysis of intrinsic cardiac neuron RNA extracts using primers specific for the insert and regions upstream and downstream of the splice (exons 1–10) failed to detect any other sequence variations ($n = 20$; data not shown).

In silico investigation using the NCBI Blast website (http://www.ncbi.nlm.nih.gov/BLAST/) has detected exon 4A in the sequence of *R. norvegicus* chromosome 1 whole genome shotgun supercontig. The sequence (6197390–6197476) is located within the region of intron 4 of the neuronal nicotinic acetylcholine receptor α7 (Chrna7) and is 413 bases downstream from the 3′ end of exon 4 (6197890) of the α7 subunit. An 87-base sequence (31346–31432) with 85% homology to the rat exon4A was also found in the mouse genome (chromosome 7) and mapped to intron 4 of the mouse α7 subunit exactly 415 bases downstream from the 3′ end of exon 4 (30932). Conservation of the sequence and position of the α7-2 sequence in the rodent genome suggests that this isoform is not particular to the rat.

Given that α7 subunits have been detected in non-neuronal cells, it seemed prudent to test for the expression of α7-2 at the single-cell level. Intrinsic cardiac neurons were isolated and probed for α7-2 expression using single-cell RT-PCR techniques similar to those reported previously (Zhang and Cuevas, 2002). To facilitate the detection of the α7-2 splice variant, a set of primers (α7-P4) (Table 1) was designed with the forward primer specific for the α7-2 isoform. A product of the predicted size for α7-2 was detected in five of seven intracardiac neurons tested (Fig. 5A), which is similar to numbers reported previously in intrinsic cardiac neurons for the α7 subunit using single-cell RT-PCR (Poth et al., 1997).

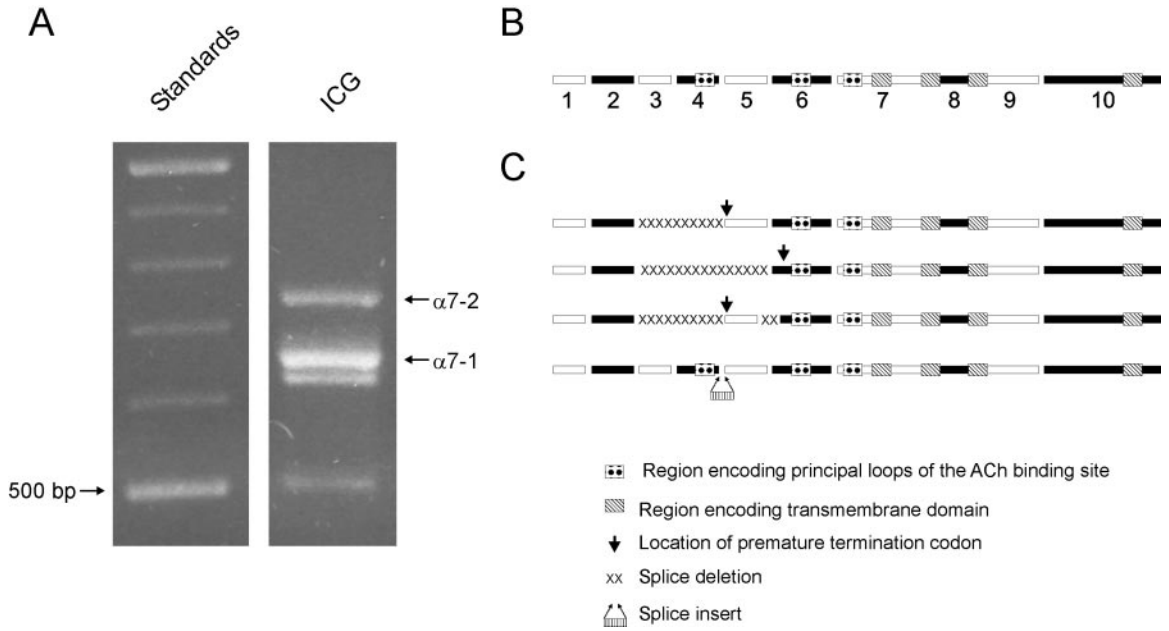

Fig. 1. Detection of multiple splice forms of the α7 neuronal nicotinic receptor subunit in rat intracardiac neurons. A, RT-PCR amplification of RNA extracts from rat intracardiac ganglia using the α7 subunit-specific primers α7-P1. Arrows, bands representing the conventional α7 gene product (α7-1) and the new sequence variant (α7-2). The 500-bp marker of a 100-bp standard ladder is indicated. Representation of α7-1 subunit transcript (B) and other splice forms of the α7 subunit (C) detected in intrinsic cardiac neurons are shown. Regions encoding the principal loops contributing to the ACh binding site and the transmembrane domains are marked relative to the exon structure. Deletions and the insertions resulting in the sequence variations are also shown (C).

Cloning and sequencing of these PCR products confirmed that they represented the α7-2 subunit.

Experiments were conducted to test for the presence of α7-2 subunit mRNA in the central nervous system and in other peripheral neurons, to determine whether expression of this subunit is limited to intracardiac ganglia. Figure 5B shows the results of a representative RT-PCR experiment using primers α7-P4 on RNA extracts from neonatal rat intracardiac, superior cervical, and nodose ganglia and brain. The α7-2 transcripts were detected in both the central nervous system and in other autonomic ganglia, suggesting that expression of this transcript is not a phenomenon exclusively associated with intrinsic cardiac neurons. To compare the relative abundance of α7-1 and α7-2 isoform transcripts in the central nervous system and in peripheral ganglia, we performed RT-PCR using multiplexed α7- and α7-2–specific primers (α7-P5) (Table 1). Bands for both the α7-1 and α7-2 were detected in all tissues tested but were not observed in two of five experiments on RNA extracts from nodose ganglia (Fig. 5C). An analysis of the intensity of the α7-2 band relative to that of the α7-1 band for these tissues is shown in Fig. 5D. The α7-1 isoform was 4- to 5-fold more abundant than the α7-2 isoform in the brain, superior cervical ganglion, and intracardiac ganglion but showed 10-fold higher expression in the nodose ganglion (Fig. 5D). A control using a 1:1 mixture of α7-1- and α7-2–pCIneo plasmids exhibited a relative intensity of 1.04 ± 0.1209 (α7-2:α7-1), indicating equivalent detection sensitivities for each isoform using this quantitative method

To determine whether transcripts encoding the α7-2 isoform are translated in central and peripheral neurons, rat brain and intracardiac and superior cervical ganglia were examined for α7-2 subunit protein expression. Protein extracts from the respective tissues were analyzed by probing immunoblots with the α7-2–specific polyclonal antibody Ab 87 (Fig. 6A). A band of the predicted size for the α7-2 protein (~58 kDa) may be readily detected in protein extracts from all tissues. To confirm that this band represents the α7-2 product, immunodepletions were performed using the anti-α7 monoclonal antibody mAb 319 that binds to the large intracellular loop between transmembrane domains 3 and 4 of the α7-1 subunit (Schoepfer et al., 1990). The amino acid sequence of the α7-2 subunit peptide is expected to be identical with that of α7-1 in this region, and thus mAb 319 should immunoprecipitate both α7-1–and α7-2–containing AChRs. Immunoblot experiments were then conducted on mock-depleted and immunodepleted extracts using the anti-α7-2 polyclonal antibody Ab 87. A band of the size predicted for the α7-2 monomer (~58 kDa) was readily detectable in immunoblots of mock-depleted extracts of all three tissues (Fig. 6B). However, the levels of this product were greatly reduced in extracts immunodepleted of α7 subunits with mAb 319 (Fig. 6B). This observation confirms the expression of α7-2 in peripheral and central tissues and verifies that Ab 87 is specific for α7-2.

The ability of the α7-2 subunit to form functional homomeric ligand-gated ion channels was examined in *X. laevis* oocytes using two-electrode voltage-clamp experiments. Figure 7A shows a family of current traces evoked by ACh at the indicated concentrations from an oocyte injected with cRNA generated from the in vitro transcription of α7-1 (top traces)

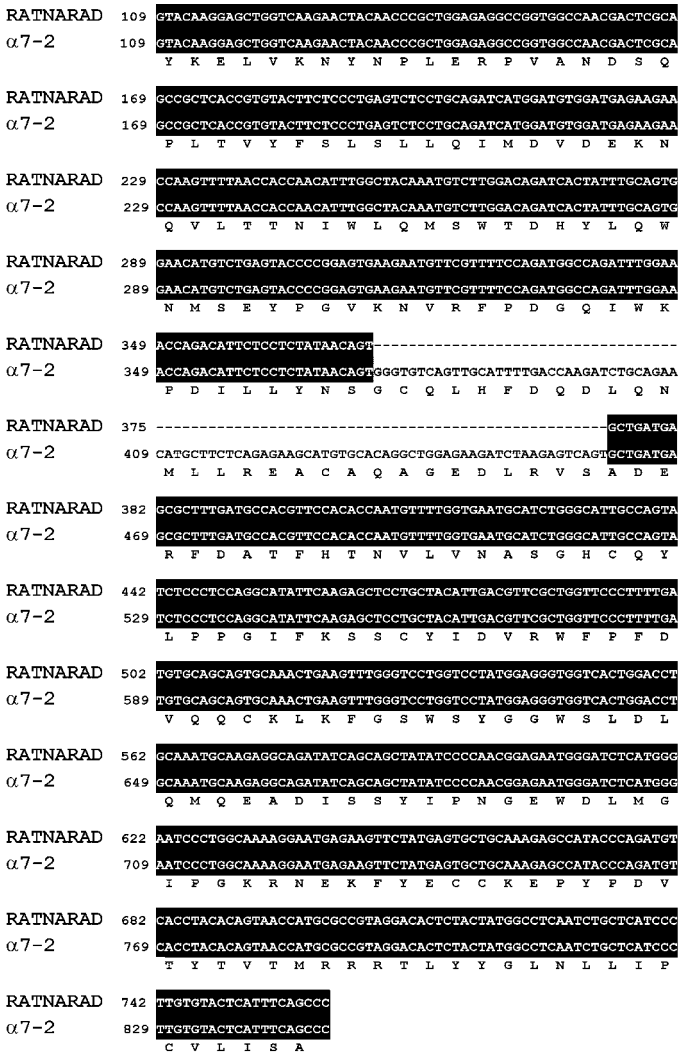

Fig. 2. Sequence of the α7-2 splice variation of the α7 gene. Sequence of insert contributing to the α7-2 variant and flanking regions as amplified by primers α7-P1, aligned to the α7-1 isoform (RATNARAD). Matching sequence is shown in white text and black background. Sequence numbering is based on the α7-1 isoform (accession number L31619). The deduced amino acid sequence is also provided.

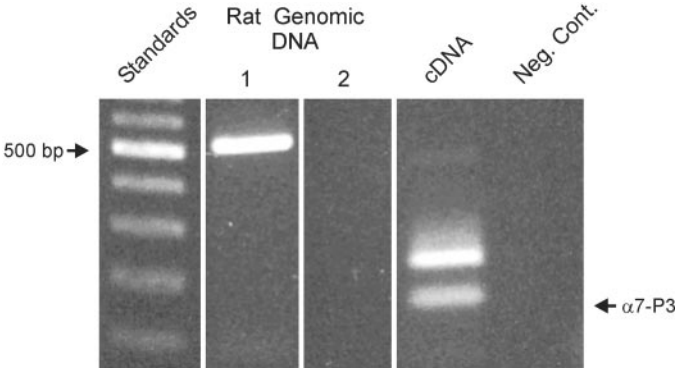

Fig. 3. Identification of a novel exon in the α7 gene. PCR amplification of genomic extracts from rat liver (1 and 2) using α7-2 subunit-specific primers α7-P2 and α7-P3, respectively. Amplification of α7-2 cDNA (cDNA) using both the α7-P2 and α7-P3 primers. Right arrow, the predicted product size for α7-P3 amplification of α7-2 cDNA. Larger product represents the product amplified by the forward primer of α7-P2 and the reverse primer of α7-P3. The 500-bp marker of a 100-bp standard ladder is indicated. Negative control (Neg. Cont.) represents a PCR reaction using H_2O.

or α7-2 (bottom traces) DNA templates. A plot of the mean concentration-response relationship for ACh activation of α7-2 homopentamers is shown in Fig. 7B ($n = 5$). A fit of the data using the Hill equation indicates that the α7-2–nAChRs were half-maximally activated by 80 μM ACh and that maximal activation occurs by 1 mM ACh. In contrast, in oocytes injected with α7-1 cRNA, ACh-evoked currents were half-maximally activated at 248 μM ACh, with maximal activation by 3 mM ACh (Fig. 7B) ($n = 5$). The Hill coefficients were 1.0 and 1.3 for α7-2 and α7-1, respectively. These data indicate that the α7-2 subunit is capable of forming functional AChRs in *X. laevis* oocytes. Moreover, α7-2–nAChRs are markedly more sensitive to ACh than α7-1–nAChRs.

One of the distinct characteristics of α7-nAChRs is their high affinity for αBgt. To determine whether sensitivity to αBgt is preserved in α7-2–nAChR, ACh-evoked currents

```
α7-2      308   GGAGTGAAGAATGTTCGTTTTCCAGATGGCCAGATTTGGAAACCAGACATTCTCCTCTAT
α7-gene   6197954 GGAGTGAAGAATGTTCGTTTTCCAGATGGCCAGATTTGGAAACCAGACATTCTCCTCTAT

α7-2      368   AACAG----------------------------------------------------------
α7-gene   6197894 AACAGgtaagcacgcctgacagatgggaaacaatcttcacttgcatgcatggggcgataa

α7-2              ----------------------------------------------------------
α7-gene   6197834 agcatatttgaggattttacagaaaagctggctgtgttatctttaatttggaaccattgc

α7-2              ----------------------------------------------------------
α7-gene   6197774 tccttttgaggctttccaagtgggcagatctctgggaggctgctctgtccctctgctggt

α7-2              ----------------------------------------------------------
α7-gene   6197714 atttgtgtctaagtttaggttgtctctccttctgccagaaatgtcctgtccaaggggctg

α7-2              ----------------------------------------------------------
α7-gene   6197654 aactatagatacataaaggtgttcaccatttatagcaatgtaaagcattcttaaggcagt

α7-2              ----------------------------------------------------------
α7-gene   6197594 cactttgctatctgaatggcaaccattacaacccacagaagaaggtgccagacagcatgt

α7-2      373   ----------------------------------------------------------TG
α7-gene   6197534 gcattggagactacagttaagacctaggttctcatctgacttttccccattgttcagTG

α7-2      375   GGTGTCAGTTGCATTTTGACCAAG
α7-gene   6197474 GGTGTCAGTTGCATTTTGACCAAG
```

Fig. 4. Sequence of intron separating exons 4 and 4a. Sequence of the α7 gene product aligned to the α7-2 isoform (α7-2). Sequence numbering for the α7-2 is derived from that provided for α7-2 in Fig. 2, while the sequence numbering for the α7 gene corresponds to that of the *R. norvegicus* Chrna7 gene. Matching sequence is shown in white text and black background. Consensus donor (gt) and acceptor (ag) sites are shown in italics and with gray background.

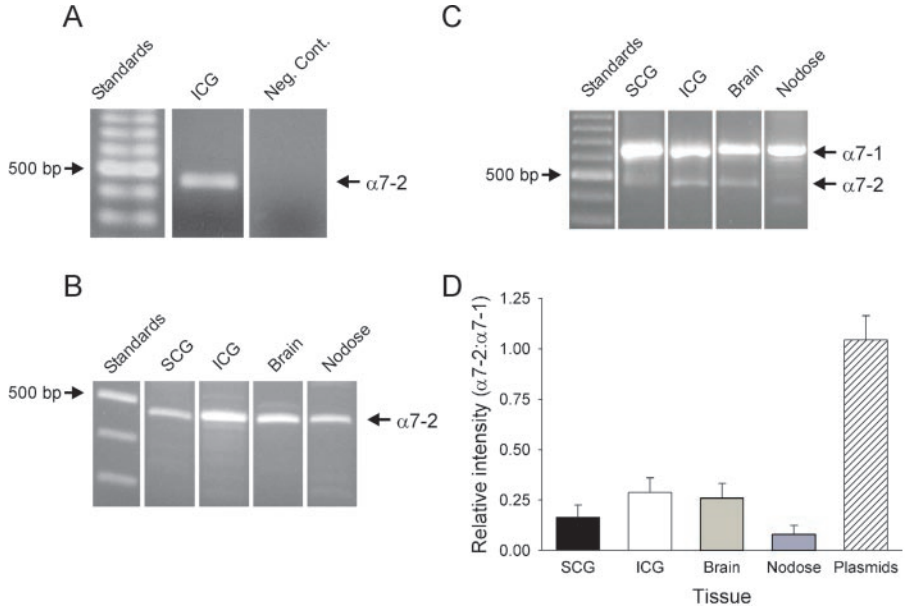

Fig. 5. The α7-2 splice variant is found in brain and in both sympathetic and parasympathetic neurons. A, RT-PCR amplification of cytoplasmic extract from a single isolated intrinsic cardiac neuron (ICG) with the α7-P4 primers. The negative control reaction was conducted using a sample of extracellular solution collected near the cell shown here. B, RT-PCR amplification of RNA extracts from rat brain and ICG, SCG, and nodose ganglia using the α7-2 subunit-specific primers α7-P4. C, RT-PCR using the α7-P5 primers on the indicated tissues. D, bar graph of the mean intensity (± S.E.M.) for the α7-2 product relative to that of the product of the α7-1 isoform obtained for each tissue ($n = 5$ for each tissue) and for a PCR amplification of a 1:1 mixture of α7-1–and α7-2–pCIneo plasmids. Arrows, the predicted size for the α7-2 (475 bp, A and B; 468 bp, C) and α7-1 (653, C only) isoforms. Standards, 100-bp ladder; the 500-bp marker is indicated.

were recorded from oocytes injected with α7-2 cRNA in the absence and presence of toxin. Figure 8A shows a family of transient currents evoked by application of 100 μM ACh (in calcium-physiological salt solution) onto a single oocyte voltage-clamped at a membrane potential of −70 mV. αBgt (50 nM) significantly ($P < 0.05$) attenuated the ACh-evoked response, and in four similar experiments, 50 nM αBgt inhibited the peak ACh-evoked current by 93 ± 3% (Fig. 8B). The inhibition by toxin was rapidly reversible, and after a 10-min wash, the ACh-evoked current recovered to near control levels (Fig. 8B). In contrast, in oocytes injected with α7-1 cRNA, αBgt block of ACh-evoked currents did not appreciably reverse over a similar time interval (data not shown). Thus, the α7-2 subunit contributes to αBgt-sensitive nAChRs, but there is a significant difference in the αBgt binding properties of α7-1–and α7-2–nAChRs subtypes.

A distinguishing attribute of α7-1 containing receptors is their rapid rate of desensitization. Figure 8C shows superimposed ACh-evoked current traces recorded from *X. laevis* oocytes injected with α7-1 and α7-2 cRNA. Unlike α7-1 homopentamers, α7-2–AChRs exhibited a slow rate of desensitization. In five similar experiments, the currents mediated by α7-1–AChRs decayed to 3.3 ± 0.6% of the peak response after 2.5 s of agonist application (Fig. 8D). However, the currents mediated by α7-2–AChRs exhibited a significantly ($p < 0.01$) slower rate of decay and were 83.3 ± 3.2% of the peak response after 2.5 s of agonist application (Fig. 8D).

Discussion

The principal finding reported here is the discovery of a novel α7 nicotinic receptor subunit isoform that forms functional α-bungarotoxin–sensitive homomeric receptors with unique biophysical and pharmacological properties when expressed in *X. laevis* oocytes. The α7-2 isoform contributes to homopentameric nAChRs that desensitize slowly, bind αBgt in a rapidly reversible manner, and have a higher affinity for ACh than α7-1–nAChRs. This isoform is produced by the incorporation of a novel cassette exon, exon 4a, near the N terminus of the receptor. Transcripts encoding this splice

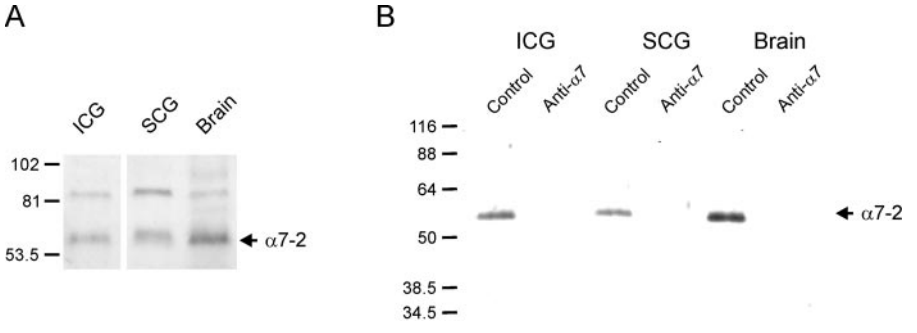

Fig. 6. Immunoblot detection of α7-2 expression in central and peripheral neurons. A, immunoblot analysis of rat ICG, SCG, and brain detergent extracts using Ab 87. B, immunoblot analysis of protein extracts from the indicated tissues either mock-depleted with rabbit–anti-rat IgG (Control) or immunodepleted with rabbit–anti-rat IgG and mAb 319 (Anti-α7). Tissues were probed for α7-2 expression using Ab 87. Each lane contained 8 μg of total protein. Protein size markers are indicated in kilodaltons.

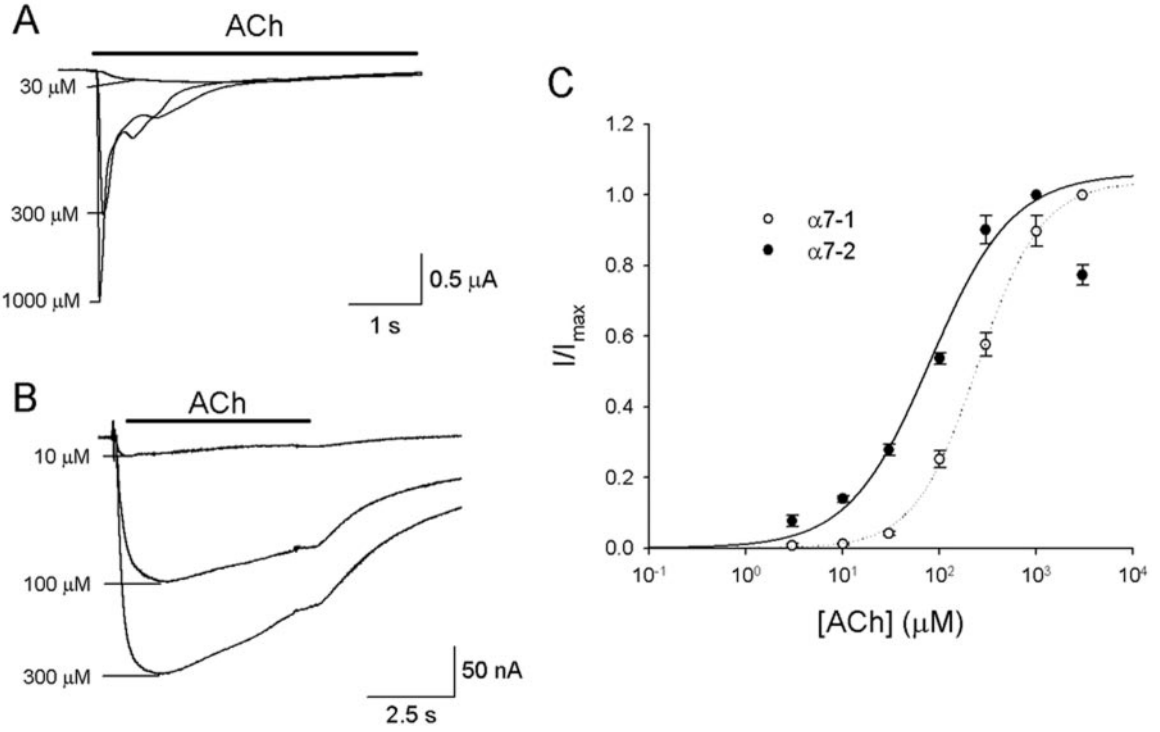

Fig. 7. The α7-2 splice variant forms functional acetylcholine receptors in *X. laevis* oocytes. Family of currents recorded in response to rapid application of ACh (5 s) at the indicated concentrations from a voltage-clamped oocyte (−70 mV) injected with either α7-1 (A) or α7-2 (B) cRNA. C, concentration-response relationship for ACh-evoked currents in oocytes injected with α7-1 (○) or α7-2 (●). Data represent mean ± S.E.M., with $n = 5$ for both conditions. Lines represent best fit to the data using the Hill equation. EC_{50} value and Hill coefficient were 248 μM and 1.3 for α7-1 and 80 μM and 1.0 for α7-2, respectively.

variant were detected in both central and peripheral neurons and were found to constitute ~20% of the total number of α7 transcripts in these tissues. Moreover, immunoblot analysis indicated the expression of the α7-2 subunit protein in the same tissues.

The existence of two functional α7 splice variants may resolve some of the long-standing controversy surrounding the structure and function of receptors containing the α7 nicotinic receptor subunit. Although several reports support the coassembly of α7 with other subunits expressed in mammals, such as α5, β2, and β3 (Girod et al., 1999; Khiroug et al., 2002), various studies using subunit-specific antibodies failed to detect the presence of non-α7 subunits in native α7-nAChRs (Schoepfer et al., 1990; Vernallis et al., 1993; Chen and Patrick, 1997; Drisdel and Green, 2000). In addition, the conventional α7 gene product, α7-1, forms functional homomeric channels when expressed in exogenous systems such as *X. laevis* oocytes and SH-EP1 cells (Couturier et al., 1990; Seguela et al., 1993; Peng et al., 1999). Although the pharmacological and electrophysiological properties of these channels were nearly identical with those of native α7-nAChRs studied in various cell types, such as rat hippocampal neurons (Alkondon and Albuquerque, 1993) and chick ciliary neurons (Zhang et al., 1994), some differences have been noted between heterologously expressed homomeric and native α7-nAChRs (Anand et al., 1993). Furthermore, electrophysiological studies in other cell types have suggested the presence of heterogeneous populations of α7-nAChRs exhibiting distinct pharmacological and biophysical properties. For example, in rat superior cervical ganglion neurons, two distinct α7-nAChR types were detected (Cuevas et al., 2000). Type I α7-nAChRs in SCG neurons desensitize rapidly, are activated by choline, and are blocked by αBgt in an irreversible manner, whereas type II α7-nAChRs desensitize slowly, are insensitive to choline and bind αBgt in a rapidly reversible manner (Cuevas et al., 2000). Likewise, it has been proposed that chick sympathetic neurons express multiple α7-nAChR subtypes, with the α7-selective antagonist methyllycaconitine discriminating between the different α7-nAChR subtypes (Yu and Role, 1998). Moreover, the observation that a sequence with 85% homology to exon 4A is also found in intron 4 of the mouse α7 subunit gene, coupled with our detection of α7-2 protein in mouse brain in preliminary studies (McCleary et al., 2002), predicts that the α7-2 subunit is probably expressed in other species.

The hypothesis that the α7 subunit exists in multiple isoforms that contribute to α7-nAChRs subtypes was first proposed by Cuevas and Berg (1998). Such α7 receptor isoforms would permit functional diversity while being consistent with studies that suggest that the α7 subunit does not combine with other nAChR subunit species. Splice variations of ligand-gated ion channels such as 5-hydroxytryptamine-3 (Bruss et al., 2000) and GABA-A (Quinlan et al., 2000) can form functional channels and affect the pharmacological

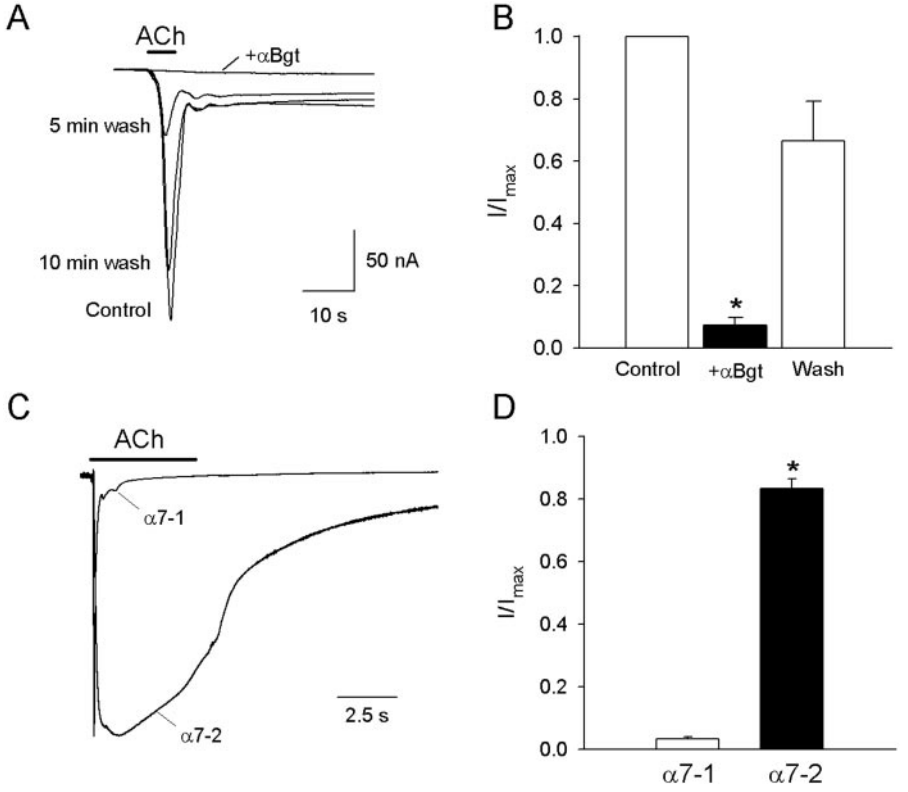

Fig. 8. α7-2–nAChRs bind α-bungarotoxin reversibly and desensitize more slowly than α7-1–nAChRs. A, ACh-evoked (100 μM) currents recorded from a voltage-clamped oocyte (−70 mV) injected with α7-2 cRNA in the absence (Control), presence of 50 nM αBgt (+αBgt), or after washout (Wash) of the toxin for the indicated time. B, bar graph of relative peak current evoked at −70 mV by 100 μM ACh in the absence (Control), presence of 50 nM αBgt (+αBgt), and after 10-min washout of toxin (Wash). Currents are normalized to control ($n = 4$). ⋆, significant difference ($P < 0.05$). C, superimposed ACh-evoked (1 mM, 5 s) current traces recorded from oocytes injected with either α7-1 or α7-2 cRNA. Currents were scaled by normalizing each current to peak response (I/I_{max}) to facilitate comparison of kinetics. D, mean relative current amplitude observed after a 2.5-s application of 1 mM ACh (−70 mV) in oocytes injected with either α7-1 or α7-2 cRNA. Currents were normalized to peak amplitude; $n = 5$ for both conditions; ⋆, significant difference ($P < 0.01$).

and/or biophysical properties of the channels. However, no splice variations of nicotinic acetylcholine subunits have been identified previously to contribute to AChRs with distinct characteristics. This lack of sequence variants of nicotinic receptors is surprising, given that most genes encoding AChR subunits contain between 5 and 10 exons, and thus numerous splice possibilities exist. Reports indicate that the α4 subunit exists in two isoforms, but when these respective isoforms are incorporated into functional channels containing the β2 subunit, they are indistinguishable on the basis of their pharmacology and biophysics (Connolly et al., 1992). The α1 subunit has also been shown to exist in multiple sequence variants, but only one of these isoforms assembles functional ACh receptors (Newland et al., 1995). Previous studies have identified several splice variants of the α7 in human brain; all but one of these splice variants contained a premature stop codon (Gault et al., 1998). In bovine chromaffin cells, a splice variant of the α7 subunit has also been detected, in which the exon that codes for the M2 transmembrane domain is deleted (Garcia-Guzman et al., 1995). This splice variant does not yield functional channels when expressed in *X. laevis* oocytes, but it inhibits the expression of α7-1 homomers when coinjected with the full-length isoform. An α7 isoform with an additional exon, which arises from alternative splicing of intron 9, has also been reported in the mouse (Saragoza et al., 2003). This mRNA yields a truncated form of the α7 peptide and acts as a dominant-negative when cotransfected with the α7-1 subunit in human embryonic kidney 293T (Saragoza et al., 2003). It remains to be determined whether the α7 splice variants detected here, which contain a premature stop codon, can regulate expression of the α7-1 and α7-2 isoforms in a similar manner. None of the previously reported α7 isoforms were detected in rat neurons in the present study.

The N-terminal location of the insert within the α7-2 subunit suggests close proximity to the ACh-binding pocket. This theory is in part supported by the crystal structure of the molluscan acetylcholine-binding protein (Brejc et al., 2001). This protein is a homolog of the amino-terminal ligand-binding domain of the α7-1 subunit and thus provides insight into the putative structure of this domain. From the crystalline structure, it was determined that three principal loops (A–C) and three complimentary loops (D–F) compose the α7 acetylcholine-binding site (Brejc et al., 2001). Exon 4a is inserted between the regions that encode principal loop A and complimentary loop E. It is thus quite likely that this insertion results in significant changes to the ACh and αBgt binding domains. This hypothesis is supported by our observation that α7-2–nAChRs have higher affinity for ACh and bind αBgt in a rapidly reversible manner compared with α7-1–nAChRs.

From the results of electrophysiological studies presented here, it is probable that the α7-2 subunit contributes to the type II α7-nAChRs of mammalian autonomic neurons (Cuevas and Berg, 1998; Cuevas et al., 2000). This species of α7-nAChRs binds αBgt with high affinity and in a rapidly reversible manner. Both type II α7–nAChRs and α7-2–nAChRs are blocked by >90% by 50 nM αBgt, and this inhibition is reversed within 10 min of toxin washout (Cuevas and Berg, 1998; Cuevas et al., 2000). A second distinguishing characteristic of type II α7-nAChRs in autonomic neurons is their slow rate of desensitization. The rate of desensitization of type I α7-nAChRs, which are probably α7-1–nAChRs, is 10-fold faster than that of type II α7-nAChRs (Cuevas et al., 2000). Data shown here indicate that α7-1–nAChRs expressed in oocytes desensitize faster than α7-2–nAChRs, further supporting the theory that the α7-2 subunit contributes to type II α7-nAChR. Given that type II α7-nAChRs mediate ~50% of whole-cell nicotinic responses in intracardiac and superior cervical ganglion neurons (Cuevas et al., 2000), α7-2–nAChRs may represent a significant population of AChRs in peripheral neurons. It is interesting to note that one of the few characteristics associated with α7-null mice is dysfunction of the autonomic nervous system (Franceschini et al., 2000). The α7-knockout mouse was generated by a deletion of exons 8 to 10 of the α7 gene (Orr-Urtreger et al., 1997), which are shared by both the α7-1 and α7-2 subunits. Thus, this dysfunction may be in part caused by the loss of the α7-2–nAChR subtype in the neurons. Consistent with an important role for α7-AChRs in regulation of the cardiovascular system is the observation that the effects of nicotine on the heart are in part caused by activation of α7 receptors in autonomic neurons (Ji et al., 2002).

In conclusion, our study presents the first evidence for acetylcholine receptor functional diversity resulting from transcriptional modifications. The finding of a novel α7 nicotinic receptor subunit isoform, α7-2, may help explain the multiplicity of α7-nAChR function. The α7-2 isoform contributes to AChRs with pharmacological and biophysical properties distinct from those of α7-1–nAChRs and closely resembling those of α7-nAChRs found in intrinsic cardiac neurons and type II α7-nAChRs of superior cervical ganglion neurons (Cuevas and Berg, 1998; Cuevas et al., 2000). The presence of α7-2 transcripts and protein in peripheral and central neurons suggests that this receptor subunit may contribute to cell-to-cell signaling in both branches of the nervous system.

Acknowledgments

We thank Dr. Darwin Berg (University of California, San Diego) and Dr. Roger Papke (University of Florida) for generously providing the α7-1 constructs and Nivia Cuevas for comments on a draft of this manuscript.

References

Alkondon M and Albuquerque EX (1993) Diversity of nicotinic acetylcholine receptors in rat hippocampal neurons. I. Pharmacological and functional evidence for distinct structural subtypes. *J Pharmacol Exp Ther* **265:**1455–1473.

Anand R, Peng X, and Lindstrom J (1993) Homomeric and native α7 acetylcholine receptors exhibit remarkably similar but non-identical pharmacological properties, suggesting that the native receptor is a heteromeric protein complex. *FEBS Lett* **327:**241–246.

Azam L, Winzer-Serhan U, and Leslie FM (2003) Co-expression of alpha7 and beta2 nicotinic acetylcholine receptor subunit mRNAs within rat brain cholinergic neurons. *Neuroscience* **119:**965–977.

Berger F, Gage FH, and Vijayaraghavan S (1998) Nicotinic receptor-induced apoptotic cell death of hippocampal progenitor cells. *J Neurosci* **18:**6871–6881.

Brejc K, van Dijk WJ, Klaassen RV, Schuurmans M, van Der Oost J, Smit AB, and Sixma TK (2001) Crystal structure of an ACh-binding protein reveals the ligand-binding domain of nicotinic receptors. *Nature (Lond)* **411:**269–276.

Bruss M, Barann M, Hayer-Zillgen M, Eucker T, Gothert M, and Bonisch H (2000) Modified 5-HT3A receptor function by co-expression of alternatively spliced human 5-HT3A receptor isoforms. *Naunyn-Schmiedeberg's Arch Pharmacol* **362:** 392–401.

Chen D and Patrick JW (1997) The α-bungarotoxin-binding nicotinic acetylcholine receptor from rat brain contains only the α7 subunit. *J Biol Chem* **272:**24024–24029.

Connolly J, Boulter J, and Heinemann SF (1992) Alpha 4–2 beta 2 and other nicotinic acetylcholine receptor subtypes as targets of psychoactive and addictive drugs. *Br J Pharmacol* **105:**657–666.

Conroy WG and Berg DK (1995) Neurons can maintain multiple classes of nicotinic acetylcholine receptors distinguished by different subunit compositions. *J Biol Chem* **270:**4424–4431.

Couturier S, Bertrand D, Matter JM, Hernandez MC, Bertrand S, Millar N, Valera

S, Barkas T, and Ballivet M (1990) A neuronal nicotinic acetylcholine receptor subunit (α 7) is developmentally regulated and forms a homo-oligomeric channel blocked by α-BTX. *Neuron* **5:**847–856.
Cuevas J and Berg DK (1998) Mammalian nicotinic receptors with α7 subunits that slowly desensitize and rapidly recover from α-bungarotoxin blockade. *J Neurosci* **18:**10335–10344.
Cuevas J, Roth AL, and Berg DK (2000) Two distinct classes of functional α7-containing nicotinic receptor on rat superior cervical ganglion neurons. *J Physiol* **525:**735–746.
Dineley KT, Bell KA, Bui D, and Sweatt JD (2002) β-Amyloid peptide activates α7 nicotinic acetylcholine receptors expressed in *Xenopus* oocytes. *J Biol Chem* **277:** 25056–25061.
Drisdel RC and Green WN (2000) Neuronal alpha-bungarotoxin receptors are alpha7 subunit homomers. *J Neurosci* **20:**133–139.
Franceschini D, Orr-Urtreger A, Yu W, Mackey LY, Bond RA, Armstrong D, Patrick JW, Beaudet AL, and De Biasi M (2000) Altered baroreflex responses in α7 deficient mice. *Behav Brain Res* **113:**3–10.
Freedman R, Coon H, Myles-Worsley M, Orr-Urtreger A, Olincy A, Davis A, Polymeropoulos M, Holik J, Hopkins J, Hoff M, et al. (1997) Linkage of a neurophysiological deficit in schizophrenia to a chromosome 15 locus. *Proc Natl Acad Sci USA* **94:**587–592.
Garcia-Guzman M, Sala F, Sala S, Campos-Caro A, Stuhmer W, Gutierrez LM, and Criado M (1995) α-Bungarotoxin-sensitive nicotinic receptors on bovine chromaffin cells: molecular cloning, functional expression and alternative splicing of the α7 subunit. *Eur J Neurosci* **7:**647–655.
Gault J, Robinson M, Berger R, Drebing C, Logel J, Hopkins J, Moore T, Jacobs S, Meriwether J, Choi MJ, et al. (1998) Genomic organization and partial duplication of the human α7 neuronal nicotinic acetylcholine receptor gene (CHRNA7). *Genomics* **52:**173–185.
Girod R, Crabtree G, Ernstrom G, Ramirez-Latorre J, McGehee D, Turner J, and Role L (1999) Heteromeric complexes of α5 and/or α7 subunits—effects of calcium and potential role in nicotine-induced presynaptic facilitation. *Ann NY Acad Sci* **868:**578–590.
Ji S, Tosaka T, Whitfield BH, Katchman AN, Kandil A, Knollmann BC, and Ebert SN (2002) Differential rate responses to nicotine in rat heart: evidence for two classes of nicotinic receptors. *J Pharmacol Exp Ther* **301:**893–899.
Khiroug SS, Harkness PC, Lamb PW, Sudweeks SN, Khiroug L, Millar NS, and Yakel JL (2002) Rat nicotinic ACh receptor alpha7 and beta2 subunits co-assemble to form functional heteromeric nicotinic receptor channels. *J Physiol* **540:**425–434.
Liu Q, Kawai H, and Berg DK (2001) β-Amyloid peptide blocks the response of α7-containing nicotinic receptors on hippocampal neurons. *Proc Natl Acad Sci USA* **98:**4734–4739.
McCleary D, Gordon M, Dickey C, Severance E, Morgan D, and Cuevas J (2002) Distribution of a novel isoform of the α7 nicotinic receptor subunit in APP-PS1 transgenic mice. *Abstr Soc Neurosci* 884.16.
Newland CF, Beeson D, Vincent A, and Newsom-Davis J (1995) Functional and non-functional isoforms of the human muscle acetylcholine receptor. *J Physiol* **489:**767–778.
Orr-Urtreger A, Goldner FM, Saeki M, Lorenzo I, Goldberg L, De Biasi M, Dani JA, Patrick JW, and Beaudet AL (1997) Mice deficient in the α7 neuronal nicotinic acetylcholine receptor lack α-bungarotoxin binding sites and hippocampal fast nicotinic currents. *J Neurosci* **17:**9165–9171.
Peng JH, Lucero L, Fryer J, Herl J, Leonard SS, and Lukas RJ (1999) Inducible, heterologous expression of human α7-nicotinic acetylcholine receptors in a native nicotinic receptor-null human clonal line. *Brain Res* **825:**172–179.
Peng X, Katz M, Gerzanich V, Anand R, and Lindstrom J (1994) Human α7 acetylcholine receptor: cloning of the α7 subunit from the SH-SY5Y cell line and determination of pharmacological properties of native receptors and functional α7 homomers expressed in *Xenopus* oocytes. *Mol Pharmacol* **45:**546–554.
Poth K, Nutter TJ, Cuevas J, Parker MJ, Adams DJ, and Luetje CW (1997) Heterogeneity of nicotinic receptor class and subunit mRNA expression among individual parasympathetic neurons from rat intracardiac ganglia. *J Neurosci* **17:**586–596.
Quinlan JJ, Firestone LL, and Homanics GE (2000) Mice lacking the long splice variant of the γ2 subunit of the $GABA_A$ receptor are more sensitive to benzodiazepines. *Pharmacol Biochem Behav* **66:**371–374.
Radcliffe KA and Dani JA (1998) Nicotinic stimulation produces multiple forms of increased glutamatergic synaptic transmission. *J Neurosci* **18:**7075–7083.
Saragoza PA, Modir JG, Goel N, French KL, Li L, Nowak MW, and Stitzel JA (2003) Identification of an alternatively processed nicotinic receptor alpha7 subunit RNA in mouse brain. *Brain Res Mol Brain Res* **117:**15–26.
Schoepfer R, Conroy WG, Whiting P, Gore M, and Lindstrom J (1990) Brain α-bungarotoxin binding protein cDNAs and MAbs reveal subtypes of this branch of the ligand-gated ion channel gene superfamily. *Neuron* **5:**35–48.
Seguela P, Wadiche J, Dineley-Miller K, Dani JA, and Patrick JW (1993) Molecular cloning, functional properties and distribution of rat brain α7: a nicotinic cation channel highly permeable to calcium. *J Neurosci* **13:**596–604.
Si ML and Lee TJ (2002) Alpha7-nicotinic acetylcholine receptors on cerebral perivascular sympathetic nerves mediate choline-induced nitrergic neurogenic vasodilation. *Circ Res* **91:**62–69.
Tsuneki H, Salas R, and Dani JA (2003) Mouse muscle denervation increases expression of an alpha7 nicotinic receptor with unusual pharmacology. *J Physiol* **547:**169–179.
Vernallis AB, Conroy WG, and Berg DK (1993) Neurons assemble acetylcholine receptors with as many as three kinds of subunits while maintaining subunit segregation among receptor subtypes. *Neuron* **10:**451–464.
Villiger Y, Szanto I, Jaconi S, Blanchet C, Buisson B, Krause KH, Bertrand D, and Romand JA (2002) Expression of an α7 duplicate nicotinic acetylcholine receptor-related protein in human leukocytes. *J Neuroimmunol* **126:**86–98.
Wang H, Yu M, Ochani M, Amella CA, Tanovic M, Susarla S, Li JH, Wang H, Yang H, Ulloa L, Al-Abed Y, et al. (2003) Nicotinic acetylcholine receptor alpha7 subunit is an essential regulator of inflammation. *Nature (Lond)* **421:**384–388.
Yu CR and Role LW (1998) Functional contribution of the α7 subunit to multiple subtypes of nicotinic receptors in embryonic chick sympathetic neurones. *J Physiol* **509:**651–665.
Zhang H and Cuevas J (2002) Sigma receptors inhibit high-voltage-activated calcium channels in rat sympathetic and parasympathetic neurons. *J Neurophysiol* **87:** 2867–2879.
Zhang ZW, Coggan JS, and Berg DK (1996) Synaptic currents generated by neuronal acetylcholine receptors sensitive to alpha-bungarotoxin. *Neuron* **17:**1231–1240.
Zhang ZW, Vijayaraghavan S, and Berg DK (1994) Neuronal acetylcholine receptors that bind α-bungarotoxin with high affinity function as ligand-gated ion channels. *Neuron* **12:**167–177.

Address correspondence to: Dr. Javier Cuevas, Department of Pharmacology and Therapeutics, University of South Florida College of Medicine, 12901 Bruce B. Downs Boulevard, MDC 9, Tampa, FL 33612-4799. E-mail: jcuevas@hsc.usf.edu